

Lawrence Berkeley National Laboratory

Lawrence Berkeley National Laboratory

Title

qSF wavefront triplication in a transversely isotropic material

Permalink

<https://escholarship.org/uc/item/9d00p1mr>

Authors

Schoenberg, Michael
Daley, Thomas M.

Publication Date

2008-05-29

Peer reviewed

qSV wavefront triplexion in a transversely isotropic material

Michael Schoenberg and Thomas M. Daley, Lawrence Berkeley Lab, Berkeley CA 94720

Summary

Triplication of a wavefront, also classically known as birefringence, can and does occur in transversely isotropic (TI) media. With the growing interest in shear waves, and in particular, converted shear waves, it becomes necessary to study this phenomenon, and the bright spots that accompany it. In a plane that includes the medium's rotational symmetry axis, there may exist a range of angles within which the qSV wave, whose polarization lies in that plane, may propagate at three distinct velocities. The region of the qSV wave curve where this can occur always corresponds to the region of the qSV slowness curve where the closed qSV curve about the origin is concave. When the range of angles is small and the three arrivals are close together, the usual situation, the qSV wave within that small range will be significantly brighter than in other directions. When the range of angles is large, the two cusps of the wave surface, on the borders of the region of triplication will both be bright spots.

The existence of the triplicating region, and its location and size (in phase slowness angle space) depends on three dimensionless parameters which themselves are functions of four stiffnesses (normalized by density so they are of dimension $velocity^2$), which, in contracted Voigt notation, are c_{33} and c_{11} , the squares of the longitudinal wave speeds parallel and normal to the symmetry axis, c_{55} , the square of the transverse wave speed along the symmetry axis, and the enigmatic stiffness modulus c_{13} which does not correspond to the square of any particular wave speed. But triplication can occur only when the medium's anisotropy is 'far' from elliptical, i.e., when c_{13} is far from its 'elliptical value' of $\sqrt{(c_{11} - c_{55})(c_{33} - c_{55})} - c_{55}$.

Triplication artifacts may sometimes be seen laboratory rock physics experiments, and in long offset converted wave data, long offset VSP's, and cross-well seismic data. When it occurs, the location of triplication related bright spots can provide strong constraints on several of the parameter combinations of the medium. Wave field snapshots of triplicating qSV wavefronts in a homogeneous TI medium are shown, as well as snapshots of the triplicating wavefront refracting across an interface into an isotropic medium.

Preliminaries

With longer offsets, and with the use of shear sources in cross-well surveys, it is to be expected that triplications will appear more and more often in seismic data. The aim here is to explain the conditions for qSV wavefront triplication in transversely isotropic (TI) media, and to show the dependence of properties of the triplicating region on certain combinations of elastic moduli.

Let the 3-axis be the medium's axis of rotational symmetry. With no loss of generality, consider slowness curves and wave curves in the 1,3-plane. An approach to the variety of 'shapes' of a TI medium is as follows: consider a TI medium for which c_{11} , c_{33} and c_{55} are known. These values determine the 'anchor points' of the slowness and wave curves, the points at which these curves intersect the coordinate axes. Two useful physically appropriate (but not theoretically necessary) constraints are,

$$c_{55} < \min[c_{11}, c_{33}] \quad \text{and} \quad c_{13} > 0. \quad (1)$$

The first of these requires the transverse wave speed in the coordinate directions to be less than longitudinal wave speeds in the coordinate directions; the second requires that a uni-axial normal stress along the symmetry axis results in strain in the opposite sense perpendicular to the symmetry axis (analogous to positive Poisson's ratio in an isotropic medium). Instead of considering the variation of c_{13} directly, it is useful to consider variation in parameter E^2 , known as the 'anellipticity':

$$E^2 \equiv (c_{11} - c_{55})(c_{33} - c_{55}) - (c_{13} + c_{55})^2.$$

When $E^2 = 0$, the anisotropy of the medium is elliptical; in this case, the qSV slowness and wavefront curves are circular; no convex region, thus no triplication. There can be no triplication even for non-elliptical anisotropy, if the anisotropy is 'close' to elliptical. As E^2 increases because c_{13} decreases from its zero anellipticity value of $c_{13_0} \equiv \sqrt{(c_{11} - c_{55})(c_{33} - c_{55})} - c_{55}$, the slowness curve of the qSV slowness sheet, commonly called the qSV sheet, pulls in (the plane wave becomes faster) between the anchor points, until, for further increasing anellipticity, at a certain angle from 3-axis, the curve becomes flat in a vertical plane containing the axis of symmetry, i.e., the silhouette of the axisymmetric 'sphere-like' closed surface has a point of zero curvature. This flat spot, call it point Q , is a point of 'incipient triplication'.

Letting θ be the angle the slowness vector, call it ξ , makes with the symmetry axis, and letting ϕ be the angle the outward normal to the slowness curve (which is the physical direction of the group velocity \mathbf{v}_g) makes with the symmetry axis, then at point Q , $d\phi/d\theta = d^2\phi/d\theta^2 = 0$. For all other points, the slowness curve is convex, implying that $d\phi/d\theta > 0$. Further increase in anellipticity results in point Q bifurcating into two points of zero curvature, call them points A and B , characterized by $d\phi/d\theta = 0$, see figure 1. At point A , ϕ has a relative maximum, and at point B , a relative minimum. These then are the cusps of the triplicating wavefront shown in figure 2. Between these points is a region for which $d\phi/d\theta < 0$, a region of concavity of the slowness curve. Thus, as one moves along the slowness curve from the symmetry direction (θ increasing from 0), the angle ϕ specifying the direction of the group velocity also increases from 0, until point A is reached. After this point, since $d\phi/d\theta < 0$, increasing θ results in decreasing ϕ , until point B is reached, where $\phi_B < \phi_A$, as seen in figure 2. Now continuing

qSV wave front triplexation

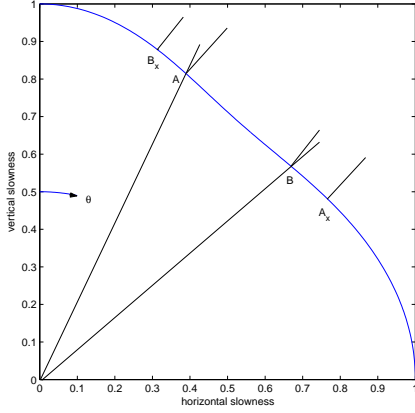


Fig. 1: Slowness curve for a triplexating TI medium. Dimensionless parameters, equation (3), are $\gamma = 1/3$, $\varepsilon_P = 1/6$ and relative anellipticity, $\mathcal{E}^2/[(1-\gamma)^2 - \varepsilon_P^2] = 7/12$.

to increase θ results in ϕ increasing, passing the value of ϕ_A , and further until as $\theta \rightarrow \pi/2$, also $\phi \rightarrow \pi/2$. The angular region defined by $\phi_B < \phi < \phi_A$ is the physical region of triplexation. The concave region defined by $\theta_A < \theta < \theta_B$ in figure 1 is the region in the slowness domain which corresponds to the outer (faster) edge of the triplexating region seen in figure 2. The full slowness region corresponding to all group velocity vectors between ϕ_B and ϕ_A is the region between B_x and A_x in figure 1.

Triplexation appears also when anellipticity is sufficiently negative, i.e., when c_{13} is larger than its zero anellipticity value. In that case, triplexation appears along the 3-axis, when

$$c_{13} > \sqrt{c_{11}(c_{33} - c_{55})} - c_{55},$$

and along the 1-axis, when

$$c_{13} > \sqrt{c_{33}(c_{11} - c_{55})} - c_{55}.$$

However, negative anellipticity is not the usual case in sedimentary basins and it cannot occur in a the medium that is long wavelength equivalent to fine isotropic layers, see (Schoenberg, 1994). For a detailed analysis of negative anellipticity triplexation, see (Schoenberg and Helbig, 1997).

The qSV dispersion relation and group velocity

The qSV dispersion relation in polar coordinates, which is the larger solution of the general qP-qSV dispersion relation, a quadratic equation on ξ^2 , with coefficients that are functions of θ , may be written,

$$F_{qSV} = c_{55}\xi^2 - \frac{1}{f_{qSV}(\cos 2\theta)} = 0, \quad (2)$$

where

$$f_{qSV}(u) = \frac{1}{2\gamma} \left[(1 - \varepsilon_P u + \gamma) - \sqrt{(1 - \varepsilon_P u - \gamma)^2 - \mathcal{E}^2(1 - u^2)} \right].$$

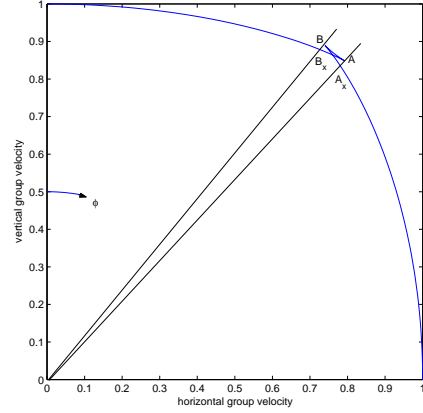


Fig. 2: qSV wavefront curve for a triplexating TI medium. Dimensionless parameters are the same in Figure 1.

Here, the dispersion relation is expressed in terms of three convenient dimensionless parameter combinations,

$$\gamma \equiv \frac{c_{55}}{(c_{11} + c_{33})/2}, \quad \varepsilon_P = \frac{(c_{11} - c_{33})/2}{(c_{11} + c_{33})/2},$$

$$\mathcal{E}^2 = \frac{E^2}{[(c_{11} + c_{33})/2]^2}. \quad (3)$$

γ is analogous to the square of the ratio of shear to compressional wave speeds in an isotropic medium. ε_P is a symmetric way of making dimensionless the difference between the squares of the longitudinal wave speeds along the coordinate axes. Note that $1 - \varepsilon_P u - \gamma > 0$ for any u , $0 \leq u \leq 1$, from the first constraint of (1). Also note that $f_{qSV}(\pm 1) = 1$.

In terms of the dispersion relation $F(\xi) = F(\mathbf{k}/\omega) = 0$, group velocity is,

$$\mathbf{v}_g \equiv \frac{d\omega}{d\mathbf{k}} = -\frac{\nabla_{\mathbf{k}} F}{\partial_{\omega} F} = -\frac{(1/\omega)\nabla_{\xi} F}{-(\mathbf{k}/\omega^2) \cdot \nabla_{\xi} F} = \frac{\nabla_{\xi} F}{\xi \cdot \nabla_{\xi} F}. \quad (4)$$

Since group velocity is parallel to the gradient of F which is always normal to contour lines of F , and the slowness curve is a contour line of F (i.e., $F = 0$), group velocity is always normal to the slowness curve. Note that $\xi \cdot \mathbf{v}_g \equiv 1$, which is the defining relation for the wave and slowness curves (or surfaces) to be polar reciprocal to one another. For the derivation of results concerning triplexation, the critical expression is for the qSV group velocity in polar coordinates,

$$\mathbf{v}_g = \frac{1}{\xi} \left[\mathbf{e}_{\xi} + \frac{\mathbf{e}_{\theta}}{\xi} \frac{\partial F_{qSV}}{\partial \theta} \right] = \frac{1}{\xi} \left[\mathbf{e}_{\xi} - \mathbf{e}_{\theta} \frac{f'_{qSV}(u)}{f_{qSV}(u)} \sin 2\theta \right], \quad (5)$$

where \mathbf{e}_{ξ} and \mathbf{e}_{θ} are the unit vectors parallel to ξ and normal to it in the θ direction, respectively, and $'$ refers to differentiation with respect to $u = \cos 2\theta$. Consequently,

$$\tan \angle(\bar{\mathbf{v}}_g, \bar{\xi}) = \tan(\phi - \theta) = -\frac{f'_{qSV}}{f_{qSV}} \sin 2\theta, \quad (6)$$

qSV wave front triplcation

is the needed relationship between ϕ and θ to decide if the slowness surface is convex ($d\phi/d\theta > 0$) or concave ($d\phi/d\theta < 0$).

Positive anellipticity wave front triplcation

Except for the rather uninteresting case when $c_{11} = c_{33}$, i.e. $\varepsilon_P = 0$, in which case the slowness curve is symmetric about the $\theta = \pi/4$ direction, one doesn't know before hand the angle of incipient triplcation. Following the very clever derivation by Peyton (1983), one finds, at incipient triplcation, relations for slowness angle,

$$\cos 2\theta_Q = \sin 2\delta_Q = \frac{\varepsilon_P}{1-\gamma} \equiv \frac{c_{11} - c_{33}}{c_{11} - c_{33} - 2c_{55}}, \quad (7)$$

where $\delta_Q = \pi/4 - \theta_Q$, and for magnitude of the slowness,

$$c_{55}\xi_Q^2 = \frac{1-\gamma}{\sqrt{(\mathcal{E}_{\text{trip}}^2)^2/4\gamma^2 + \mathcal{E}_{\text{trip}}^2/\gamma + \varepsilon_P^2}}, \quad (8)$$

which is in terms of the unknown $\mathcal{E}_{\text{trip}}^2$. For $c_{11} > c_{33}$, ε_P is positive, and thus δ_Q is positive so point Q is closer to the 3-axis than the 1-axis; when $c_{11} < c_{33}$, ε_P is negative, and point Q is closer to the 1-axis.

Substituting the values of equations (7) and (8) into dispersion relation (2) gives a cubic equation on the value of $\mathcal{E}_{\text{trip}}^2$. The appropriate root of that equation is,

$$\mathcal{E}_{\text{trip}}^2 = 2 \left(1 - \frac{2}{3}\gamma + \gamma^2 - \varepsilon_P^2 \right) \sin \left(\frac{2\psi}{3} + \frac{\pi}{6} \right) - \left(1 + \frac{2}{3}\gamma + \gamma^2 - \varepsilon_P^2 \right), \quad (9)$$

where

$$\cos \psi = - \frac{\sqrt{(1-\gamma)^2 - \varepsilon_P^2} [1 - \gamma^2 - \varepsilon_P^2]}{\left[\sqrt{1 - (2\gamma/3) + \gamma^2 - \varepsilon_P^2} \right]^3}. \quad (10)$$

A plot of $\mathcal{E}_{\text{trip}}^2/[(1-\gamma)^2 - \varepsilon_P^2]$ (which is E_{trip}^2 normalized by $E^2|_{c_{13}=-c_{55}}$, the largest value E^2 can attain) as a function of γ for fixed ε_P , shows that ε_A is relatively insensitive to ε_P and is almost linearly dependent on γ . Thus, for clarity, it is useful to form a new parameter, K , given by

$$\begin{aligned} K &\equiv \frac{\mathcal{E}_{\text{trip}}^2}{\gamma [(1-\gamma)^2 - \varepsilon_P^2]} \\ &= \frac{(c_{11} - c_{55})(c_{33} - c_{55}) - (c_{13\text{trip}} + c_{55})^2}{(c_{11} - c_{55})(c_{33} - c_{55})} \\ &\equiv \frac{2c_{55}}{(c_{11} + c_{33})} \end{aligned} \quad (11)$$

which is plotted in figure 3 as a function of γ for six values of ε_P : 0, 1/12, 1/6, 1/4, 1/3 and 5/12. As can be seen from the figure, parameter K is almost constant, with values confined to

the small range between 4/3 and about 3/2, over a wide range of γ and ε_P . In the limit as $\gamma \rightarrow 0$,

$$\frac{\mathcal{E}_{\text{trip}}^2}{\gamma [(1-\gamma)^2 - \varepsilon_P^2]} \rightarrow \frac{4}{3} \frac{\sqrt{4 - 3\varepsilon_P^2} - 1}{1 - \varepsilon_P^2},$$

and for the six values of ε_P given above, this result for vanishingly small γ yields $K = 4/3, 1.336, 1.343, 1.355, 1.372$ and 1.396 , respectively.

In any event, in terms of K which can be recovered from figure 3, the value of $c_{13\text{trip}}$ for incipient triplcation is given, from equation (11), by

$$\begin{aligned} \frac{c_{13\text{trip}}}{c_{55}} &= \frac{\sqrt{(1-K\gamma)[(1-\gamma)^2 - \varepsilon_P^2]} - 1}{\gamma} \\ &= \frac{\sqrt{(1-K\gamma)(c_{11} - c_{55})(c_{33} - c_{55})}}{c_{55}} - 1. \end{aligned} \quad (12)$$

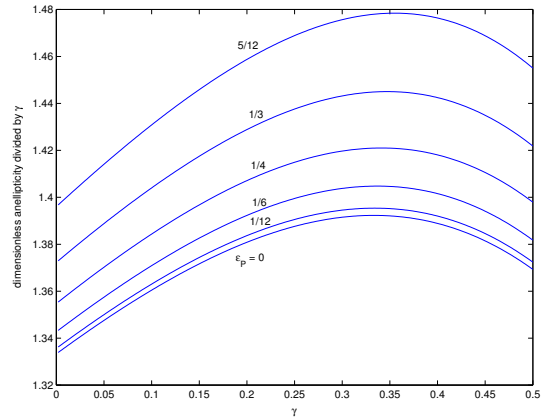


Fig. 3: Almost constant parameter K , the relative anellipticity at incipient triplcation divided by γ , as a function of γ , for values of ε_P .

Numerical modeling and discussion

Figures 4 and 5 show snapshots (calculated from staggered grid finite difference code) of the wave field generated by an explosive point source in a TI medium with specific density 1 and with density normalized elastic moduli given by $c_{11} = 3.5$, $c_{33} = 2.5$, $c_{55} = 1.0$ and $c_{13} = 0.25$, units in $(\text{km/s})^2$. These give rise to dimensionless parameters $\gamma = 1/3$, $\varepsilon_P = 1/6$ and relative anellipticity $\mathcal{E}^2/[(1-\gamma)^2 - \varepsilon_P^2] = 7/12$ as given in the caption of figure 1.

For those anchor points, the value of K (from figure 3 is 1.405, giving a value of relative anellipticity at incipient triplcation of $0.468 < 7/12$ so this medium has a triplcating qSV wave front. This is seen in figure 4, a snapshot of the wave field's horizontal particle velocity at 100 ms. The compressional and shear wave speeds in the 3-direction are $\sqrt{2.5} \sim 1.581$ and 1 km/s, respectively. The point source is located 150 m above an isotropic half-space so the compressional wave has just reached the interface.

qSV wave front triplexation

The triplexations of the qSV wave front are clear and relatively bright, the shape the same as that given in figure 2, although the region of triplexation is so small that individual arrivals are not discernible.

The isotropic medium below the interface has specific density 1 and compressional and shear wave speeds of $\sqrt{3} \sim 1.732$ and 1 km/s, respectively. Figure 5, a snapshot at 250 ms, shows bright spots on the qS \rightarrow S wave front, in the isotropic medium, as well as the edges of the qS \rightarrow P converted wave.

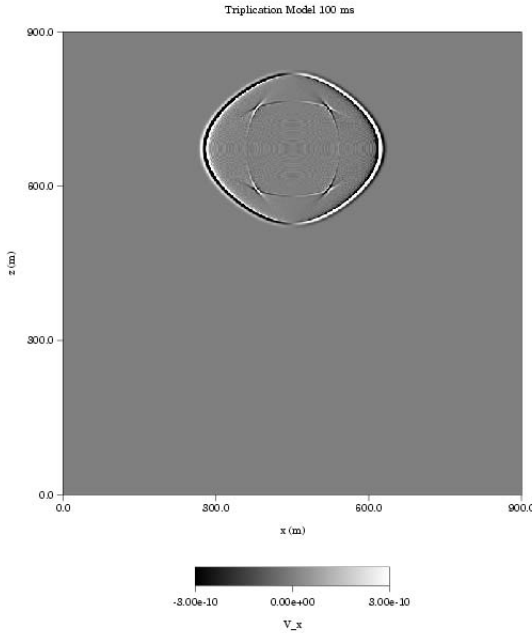


Fig. 4: Snapshot at 100 ms of the particle velocity in the 1-direction of the wavefield due to an explosive point source in a TI medium with parameters as given in figure 1.

Conclusions

Triplexation of the qSV wave front is by no means a ubiquitous phenomenon. Yet it does occur in various situations. Strict criteria for the occurrence of triplexation has been given in terms of the range of c_{13} as a function of the other relevant elastic stiffnesses. This has been approached, for positive anellipticity media, by finding the required value of anellipticity, related to, but a symmetric version of, $\epsilon^T - \delta^T$ (where superscript T refers to Thomsen (1986) parameters), needed as a function of, primarily, γ , the ratio of c_{55} to the mean of c_{11} and c_{33} , and, weakly, of ϵ_P , the symmetric version of ϵ^T . Symmetric parameterization is necessary since the occurrence of the phenomenon depends on the values of c_{11} and c_{33} in a symmetrical fashion.

Because of the small range of K in figure 3, a reasonable rule of thumb is that K is within 3% of 1.39, and most likely, considerably less, so that any positive anellipticity earth material with known anchor points will triplexate, or not, depending on

whether or not its value of c_{13}/c_{55} is less than, or greater than

$$\frac{\sqrt{(1 - 1.39\gamma) [(1 - \gamma)^2 - \epsilon_P^2]}}{\gamma} - 1.$$

Note that for $\gamma \sim 1/3$, an actual error of 3% would cause an error of only about 4% in c_{13} .

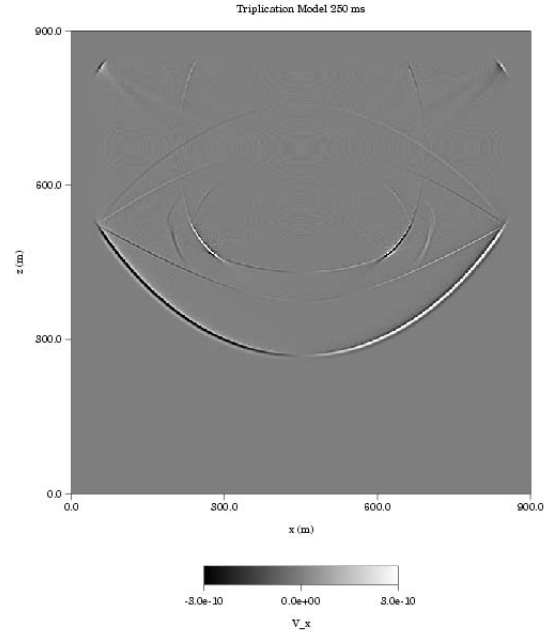


Fig. 5: Snapshot at 250 ms after the source which is located 150 m above an underlying halfspace of an isotropic medium of specific density 1, compressional speed 1.732 km/s and shear speed 1 km/s.

The bright spots associated with triplexating wave fronts are also of interest, as they could confuse the picture one tries to form of bright spots associated with reflectivity. However, the detection of qSV triplexating wavefront bright spots will also give information as to the shape of the slowness surface of the medium in which the triplexating wavefront occurs, from an estimate of anellipticity to an estimate of the difference between c_{11} and c_{33} just from knowing the angular location of the triplexating region.

References

- Peyton, 1983, Elastic wave propagation in transversely isotropic media: Martinus Nijhoff Publishers.
- Schoenberg, M. 1994, Transversely isotropic media equivalent to thin isotropic constituent layers: Geophys. Prosp., **42**, 885-915.
- Schoenberg, M. and Helbig, K., 1997, Orthorhombic media: Modeling elastic wave behavior in a vertically fractured earth: Geophysics, **62**, 1954-1974.
- Thomsen, L., 1986, Weak elastic anisotropy: Geophysics, **51**, 1954-1966.